

NEW APPLICATIONS OF SHAPE DESIGNED COMPLEMENTARY SIGNALS FOR TESTING OF ANALOG SECTIONS IN ELECTRONIC EMBEDDED SYSTEMS

Dariusz Załęski¹, Bogdan Bartosiński, Romuald Zielonko

¹ Gdansk University of Technology, Faculty of Electronics, Telecommunication and Informatics, Department of Optoelectronics and Electronic Systems, Poland, dzaleski@eti.pg.gda.pl, bbart@eti.pg.gda.pl, zielonko@eti.pg.gda.pl

Abstract: The article concerns the implementation of shape designed complementary signals in BISTs used in mixed-signal embedded systems for testing of their analog sections. The essence of the proposed method is stimulation of the tested circuit with a complementary signal of a designed particular shape, whose parameters are matched to the nominal position of circuit transfer function poles. The paper presents results of simulation research and practical verification of the method in a microsystem based on an ADuC814 microcontroller.

Keywords: electronic embedded systems, complementary signals, Built-In Self-Testers.

1. INTRODUCTION

The development and expansion of electronic embedded systems is observed during the last years. These systems are controlled by intelligent units that are realised usually as microcontrollers.

The dominant group of electronic embedded systems are mixed-signal systems. Analog signals from sensors are conditioned in a system analog section and afterwards converted into a digital form and processed in a digital section of the electronic embedded system.

At present, two classes of methods for testing of electronic circuits such as *test buses* and *Built-In Self-Testers* (BISTs) are developed.

The test bus, compliant with the IEEE 1149.1 standard, solves many problems with testability of digital devices. The standard is based on the boundary scan technique and provides the ability to test digital circuits at the chip level, board level and system level.

Testing of mixed-signal systems is possible by the IEEE Standard 1149.4, which is an extension of IEEE Std 1149.1 and is fully compatible with it in the digital part of the device. Added structures permit testing of the mixed-signal core of a circuit and testing of analog elements situated between bus-equipped circuits. The main disadvantage of the analog test bus are only two lines dedicated for testing of analog circuits, but the bus is effective in co-operation with BISTs.

BISTs are dedicated for specific application and appear as excessive structures that are entered into ICs, electronic packets or systems. Unfortunately, this solution results in

system redundancy and increasing costs. Recently, there are possibilities for software realisation of BISTs basing only on internal resources of a microcontroller.

Nowadays, new generations of microcontrollers (e.g. AT91SAM, PIC18F452, ADuC814) are equipped with many advanced on-chip peripherals such as: ADCs, DACs, timers/counters, communication interfaces (UART, I²C, SPI), analog comparators, etc. Numerous and simultaneously limited groups of microcontroller internal resources allow to create simple and specific BISTs without any requirement for additional external resources.

The realisation of BISTs basing on shape designed stimulating signals, called complementary signals (CSs), is proposed in the paper. The presented approach utilizes internal resources existing in an electronic embedded system microcontroller that controls the system and extends its functions to self-testing of the system analog section.

Utilization of CSs for testing was introduced in mid-80's [1], but the technology level at that time impeded broad application of CS BISTs. Nowadays, electronic embedded systems can be easily equipped with CS BISTs due to the simplicity of CSs generation and processing of the response of the tested circuit.

2. THE IDEA OF THE METHOD

The essence of the presented method is stimulation of a Circuit Under Test (CUT) with CS – the signal of specially designed shape. The parameters of the stimulation are exactly matched to poles of the CUT transfer function poles [2, 3].

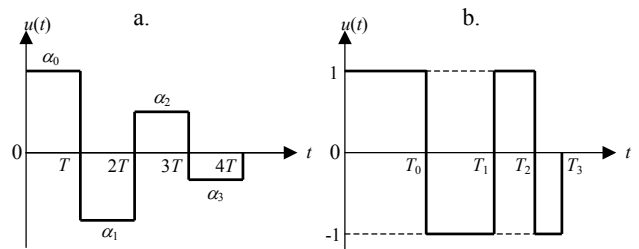


Fig. 1. Third order complementary signals (a) α -parameters (fixed duration of impulses) and (b) T -parameters (fixed level of impulses)

The CS consists of a sequence of $(n+1)$ impulses with alternating polarisation (Fig. 1), where n is the number of CUT transfer function poles. The first impulse from the

sequence drives the stimulated CUT into an initial state whereas the remaining impulses compensate it in a manner, that the CUT response reaches zero and remains at that level.

The vanishing of CUT response, remaining at zero level after the end of stimulation (Fig. 2) unambiguously proves that the localization of tested circuit transfer function poles and its frequency response are correct. The CUT nonzero response after the end of stimulation means that the localization of its transfer function poles is improper as the result of fault (Fig. 2).

In general, the CS can be described by the expression

$$u_n(t) = \alpha_0 E(t) - \alpha_1 E(t - T_0) + \dots + (-1)^n \alpha_n E(t - T_{n-1}), \quad (1)$$

where: $E(t - T_i)$, $i = 0, 1, \dots, n$ – some function defined in the interval $[T_i, T_{i+1}]$ and equal to zero outside it,
 α_i , T_i – amplitude and time parameters of the signal,
 n – number of poles, signal order.

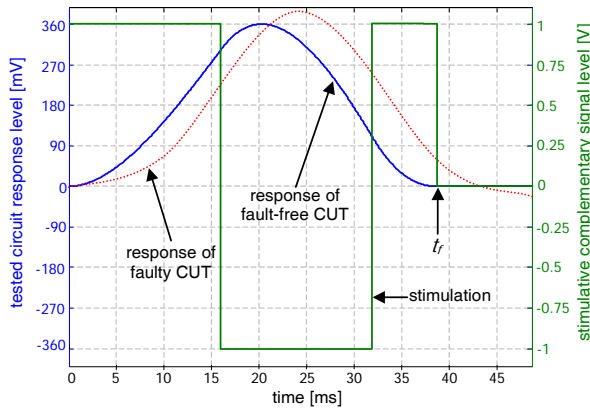


Fig. 2. The exemplary CUT response to matched T_i -parameter CS for a fault-free circuit (solid line) and a faulty one (dotted line)

According to the equation (1) there are two types of CSs:

- α_i -parameter signals with variable levels of pulses and fixed pulse duration,
- T_i -parameter signals with variable pulse duration and fixed level of pulses.

The shape of each type of CSs is described by $E(t)$ function (e.g. constant, ramp, polynomial, etc.).

The complementary matched signal stimulates the CUT and sets its output to zero after the end of stimulation t_f . This criterion allows to define the relation between the CUT transfer function poles and parameters of CS. The tested circuit response is derived from the state-space analysis with limiting the consideration to single-input single-output linear time-invariant strictly proper stable circuits, the transfer function of which is given by

$$G(s) = \frac{b^m s^m + \dots + b_1 s + b_0}{s^n + a_{n-1} s^{n-1} + \dots + a_1 s + a_0}, \quad (2)$$

where: n – number of poles, m – number of zeros, $n > m$, and whose frequency characteristics are determined by their transfer function poles. These circuits are represented by a numerous class of low-pass and band-pass circuits whose transfer functions do not have zeros or zeros of the transfer

function are equal to zero and whose transfer function is given by the following formulas or their combination:

$$\frac{1}{s + \omega_n}, \quad \frac{\omega_n^2}{s^2 + \frac{\omega_n}{Q}s + \omega_n^2}, \quad \frac{\frac{\omega_n}{Q}s}{s^2 + \frac{\omega_n}{Q}s + \omega_n^2}. \quad (3)$$

The above formulas define a broad class of low-pass and band-pass active and passive filters and also band-pass LC filters. These circuits can be described in the state-space form with canonical state equations [3]:

$$\begin{aligned} \dot{x} &= Ax + Bu, \\ y &= Cx, \end{aligned} \quad (4)$$

where: x – state vector, y – circuit response, A – state matrix
 B – input-to-state matrix, C – state-to-output matrix.

The state vector $x(t_f)$, which is the result of state equations (4), can be expressed at moment t_f of finishing of CS with stimulation $u(t)$ and matrix e^{At} in the following way

$$x(t_f) = e^{A(t_f - t_0)} x(t_0) + \int_{t_0}^{t_f} e^{A(t_f - \tau)} Bu(\tau) d\tau. \quad (5)$$

The CUT response vanishes for time $t \geq t_f$ if the state vector $x(t_f)$ has zero value. Equating to zero the formula (5) and assuming zero initial conditions $x(t_0) = 0$ and A is not a singular matrix, there were gained, for α_i -parameter signals, these relations between localization of the tested circuit transfer function poles and α_k signal parameters:

$$\begin{aligned} \alpha_1 &= -\sum_{i=1}^n \exp(s_i T), \\ \alpha_2 &= +\sum_{i=1}^{n-1} \sum_{j=i+1}^n \exp(s_i + s_j), \\ &\vdots \\ \alpha_n &= (-1)^n \exp\left[\sum_{i=1}^n \exp(s_i T)\right]. \end{aligned} \quad (6)$$

Formulas (6) are used for the design of α_i -parameter signals for nominal localization of the transfer function poles [3].

The main disadvantage of α_i -parameter signals lies in the technique of their generation – a high-speed DAC with high resolution is required.

The T_i -parameter signals do not have this shortcoming. Basing on state-space modeling, the following relation between nominal localization of the tested circuit poles and T_k signal parameters was obtained:

$$\begin{aligned} \sum_{k=0}^{n-1} 2(-1)^k e^{-s_1 T_k} + (-1)^n e^{-s_1 T_n} - 1 &= 0, \\ \sum_{k=0}^{n-1} 2(-1)^k e^{-s_2 T_k} + (-1)^n e^{-s_2 T_n} - 1 &= 0, \\ &\vdots \\ \sum_{k=0}^{n-1} 2(-1)^k e^{-s_n T_k} + (-1)^n e^{-s_n T_n} - 1 &= 0. \end{aligned} \quad (7)$$

The given simultaneous equations (7) are a set of n non-linear equations with n variables T_k , which represent the finishing moment of the k -th CS impulse. Values of T_k variables are dependent on nominal localization of poles s_i and also on the assumed value of duration T_0 of the first impulse.

The simultaneous equations (7) shown above cannot be solved analytically. They can only be solved by application of numerical computations.

3. SIMULATION RESEARCH

Metrological properties of the presented diagnostic method were determined for 2nd and 4th order Butterworth low-pass filters, whose parameters are presented in Table 1. The threshold value of fault detection for given filters was assumed at the level of $U_{Th} = \pm 5$ mV of their response.

Table 1. Parameters of the examined 2nd and 4th order low-pass filters.

parameter	2 nd order LPF	4 th order LPF
f_c	10 Hz	
ω_n	62.83 rad/s	
s_1, s_2	$44.4288 \pm 44.4288i$	$-58.0491 \pm 4.0447i$
s_3, s_4	—	$-24.0447 \pm 8.0491i$
Q_1	0.707	0.541
Q_2	—	1.307
configuration	inverting	non-inverting

The transfer functions of the given filters are described by the following formulas:

$$G_1(s) = \frac{3947.84}{s^2 + 88.86s + 3948}, \quad (8)$$

$$G_2(s) = \frac{15.59 \cdot 10^6}{(s^2 + 116.1s + 3948)(s^2 + 48.09s + 3948)}. \quad (9)$$

The investigated filters were stimulated with both types of CSs, whose parameters are given in Table 2, 3.

Table 2. Parameters of matched CSs for 2nd order low-pass filter.

parameter	T_i -parameter CS	α_i -parameter CS
T_0, T	15.916 ms	
T_1	31.884 ms	—
T_2	38.667 ms	—
t_f	38.667 ms	47.747 ms
α_0	—	1 V
α_1	—	-0.7497 V
α_2	—	0.2431 V

Table 3. Parameters of matched CSs for 4th order low-pass filter.

parameter	T_i -parameter CS	α_i -parameter CS
T_0, T	15.916 ms	
T_1	37.393 ms	—
T_2	57.185 ms	—
T_3	70.397 ms	—
T_4	75.027 ms	—
t_f	75.027 ms	79.58 ms
α_0	—	1 V
α_1	—	-1.5587 V
α_2	—	1.2283 V
α_3	—	-0.4722 V
α_4	—	0.07331 V

The influence on the method's detection accuracy has been analyzed for the following factors:

- duration of the first CS impulse,
- improper values of impulse levels,
- improper duration of CS impulses,
- the rise and fall time of CS impulses,
- the presence of Gaussian noise interference.

The simulated response of a given investigated fault-free low-pass filter, whose parameters are described in Table 1, to the matched α_i -parameter CS is shown in Fig. 3.

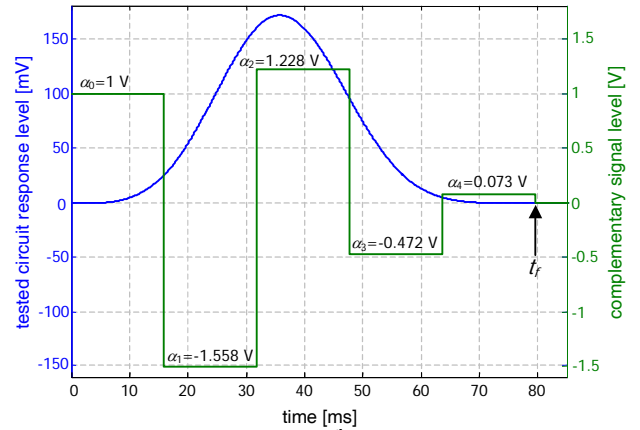


Fig. 3. The response of faultless 4th order Butterworth low-pass filter to α_i -parameter CS

As seen in Fig. 3, the simulated response of the tested fault-free filter is equal to zero at moment t_f and remains at this level for $t > t_f$.

3.1 The response sensitivity to deviations of the Q -factors and cut-off angular frequency ω_n

The result of simulation research on the influence of deviations of Q -factors in range of $\pm 50\%$ on the response of 2nd and 4th order filters $y(t_f, \alpha_i) = f(\Delta Q)$ which were stimulated with α_i -parameter CSs, is presented in Fig. 4.

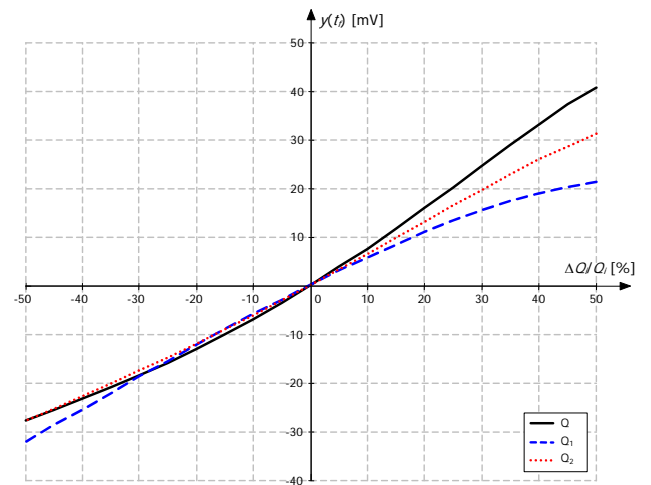


Fig. 4. The response of tested low-pass filters as a function of Q -factors for α_i -parameter CSs.

The considered relation $y(t_f, \alpha_i) = f(\Delta Q)$ is monotonic. For the assumed threshold level of faults detection at

$U_{Th}=\pm 5$ mV, a Q -factor deviation of several percent can be discovered.

Functions $y(t_f, T_i)=f(\Delta Q_i)$ for T_i -parameter CSs (Fig. 5) are monotonic for the 4th order filter and enable to detect the same level of change of Q -factors as for α_i -parameter signals. However, it is impossible to discover the Q -factor deviation in the range of $0\% < \Delta Q/Q < 40\%$ for the 2nd order filter, because the non-monotonic function $y(t_f, T_i)=f(\Delta Q)$ reaches its local minimum for $\Delta Q/Q \approx 20\%$.

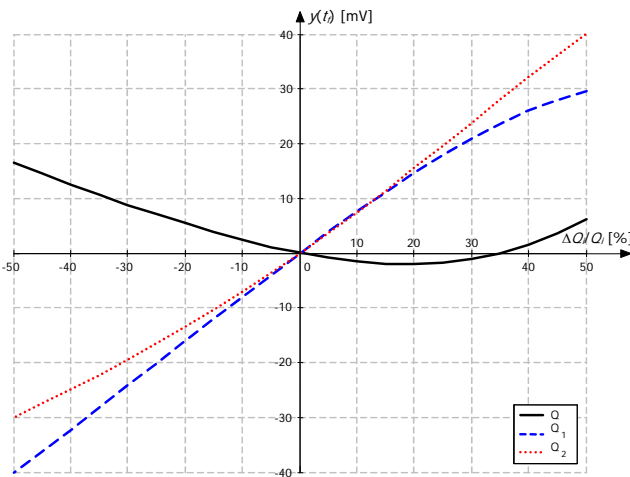


Fig. 5. The response of tested low-pass filters as a function of Q -factors for T_i -parameter CSs.

During the next stage of simulation research the influence of cut-off angular frequency ω_n deviation in the range of $\pm 50\%$ on the responses of 2nd and 4th order filters $y(t_f, \alpha_i)=f(\Delta \omega_n)$ was analyzed for α_i -parameter CSs (Fig. 6) and T_i -parameter ones (Fig. 7).

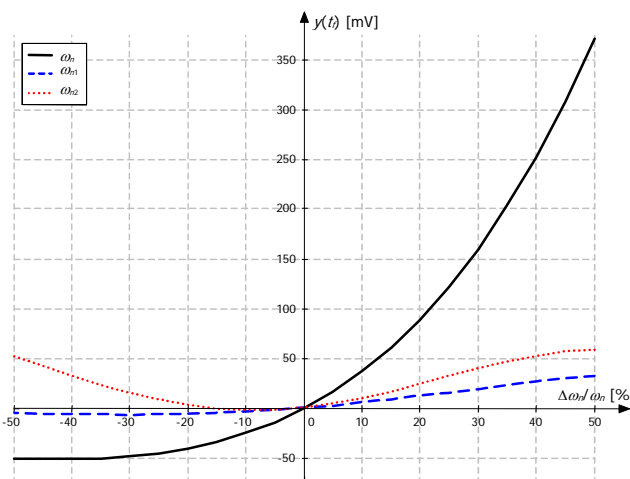


Fig. 6. The response of tested low-pass filters as a function of cut-off angular frequency ω_n for α_i -parameter CSs.

The range of response variation of the 2nd order filter is monotonic and wider than for the 4th order one. The high slope of the $y(t_f, \alpha_i)=f(\Delta \omega_n)$ curve for 2nd filter allows to detect a change of the cut-off angular frequency ω at the level of about $\pm 2\%$.

The deviation of the cut-off angular frequency ω_n can be detected at a level of about 5% for the 4th order filter at $\Delta \omega_n/\omega_n \geq 0$, whereas for $\Delta \omega_n/\omega_n < 0$ at a level of about -15%.

The $y(t_f, T_i)=f(\Delta \omega_n)$ function has the highest slope for the 2nd order filter stimulated with T_i -parameter CS, which is similar to the situation obtained for the α_i -parameter one. The response sensitivity to alteration of the cut-off angular frequency ω_n is the lowest for the first section of the 4th order filter and allows to detect the deviation of ω_n at the level of about $\pm 5\%$ and the highest for the 2nd order filter with the level of about $\pm 2\%$.

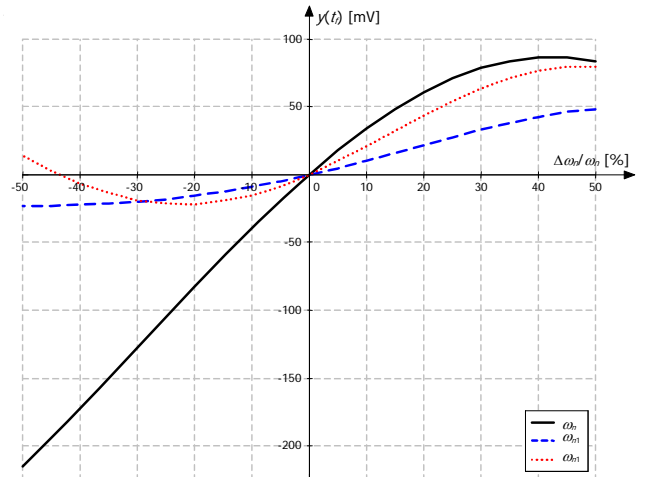


Fig. 7. The response of tested low-pass filters as a function of cut-off angular frequency ω_n for T_i -parameter CSs.

The simulation research does not show an advantage of any type of applied CSs. In order to this, the optimal complementary test signal has to be chosen for a given transfer function of the tested circuit and for particular investigated parameter.

3.2 The influence of duration of the first CS impulse on the response level

The duration of the first impulse T, T_0 (denoted as ΔT) in CS is one of factors which alter the response level of the CUT in the moment t_f and, at the same time, the method sensitivity to detection of displacement of transfer function poles caused by CUT malfunction.

The influence of duration ΔT on the tested circuit response $y(t_f)=f(\Delta T)$ was investigated for $\Delta Q/Q=\pm 10\%$ and $\Delta \omega_n/\omega_n=\pm 10\%$ and with variable ΔT in range $0.5 < \Delta T/T < 2$. Afterwards, the CUT (in this case 2nd order Butterworth low-pass filter) was stimulated with CSs matched to the nominal position of its transfer function poles for particular values of ΔT .

The nominal duration of the CS first impulse is calculated for both signal types as the reciprocal of magnitude of transfer function pole with the lowest angular frequency.

The relationship $y(t_f)=f(\Delta T)$ is presented for an α_i -parameter CS in Fig. 8, while for a T_i -parameter one in Fig. 9.

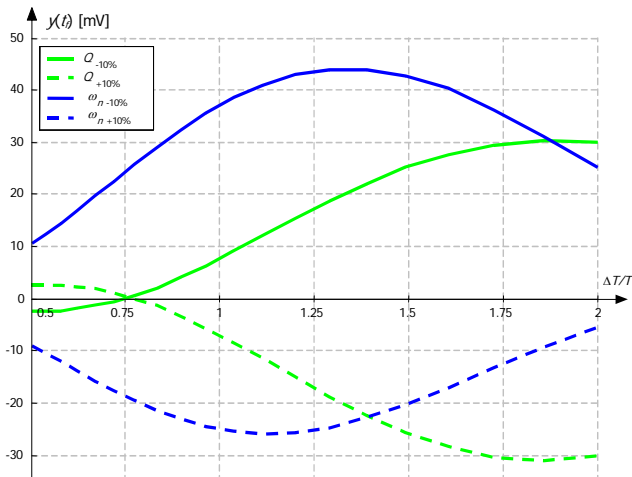


Fig. 8. The response of 2nd order low-pass filter as a function of duration of CS first impulse for α -parameter CS.

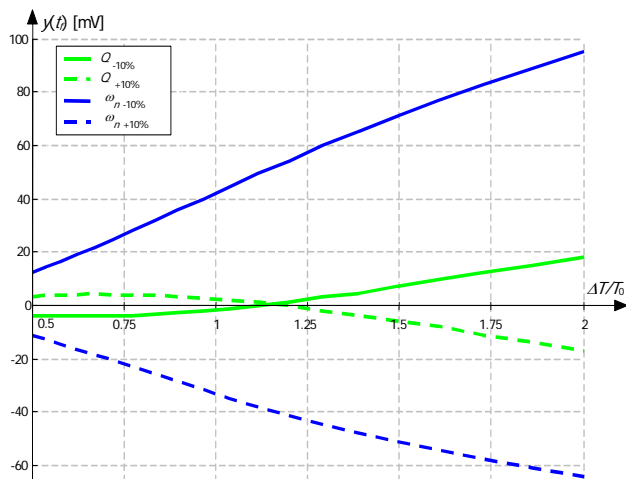


Fig. 9. The response of 2nd order low-pass filter as a function of duration of CS first impulse for T_i -parameter signal.

As seen in the above figures, the function $y(t_f, \alpha_i) = f(\Delta T)$ is non-linear and non-monotonic for the α -parameter signal. The function extrema appear for ω_n and Q -factor at different values of $\Delta T/T$, which enables to adjust the best sensitivity for the detection of deviation of a given parameter (ω_n or Q).

The function $y(t_f, T_i) = f(\Delta T)$ is monotonic and nearly linear for the T_i -parameter CS for the presented range of $0.5 < \Delta T/T < 2$, but for a greater value of $\Delta T/T$ the function $y(t_f, T_i) = f(\Delta T)$ saturates.

The level of filter response increases with an increase of the duration of the CS first impulse ΔT_0 , which can be used for improvement of the method's sensitivity at the cost of longer testing time.

3.3 The influence of improper values of CSs impulses on accuracy of the method

Imprecise impulses levels of CSs lead to non-zero value of tested fault-free circuit response in the moment t_f .

This relation is illustrated with the 2nd order filter for α -parameter (Fig. 10) and T_i -parameter CSs (Fig. 11) for a variable level of each impulse in the range of $\pm 25\%$ of their nominal levels.

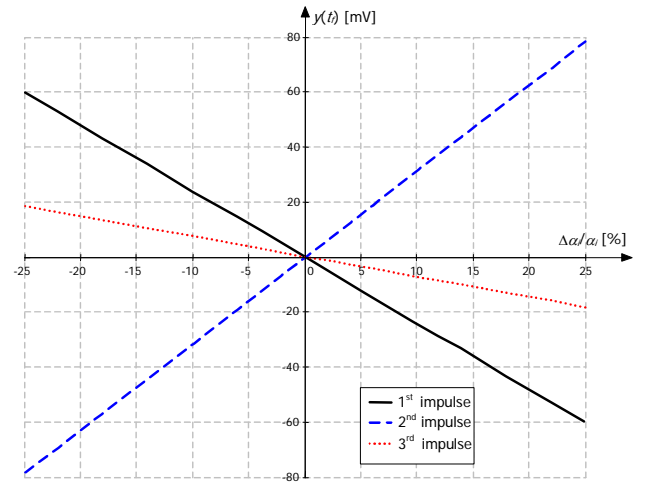


Fig. 10. The response of 2nd order filter as a function of imprecise levels of impulses for α -parameter CS.

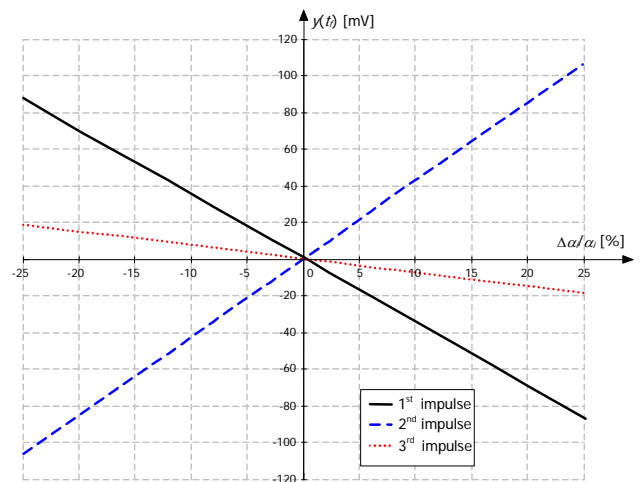


Fig. 11. The response of 2nd order filter as a function of imprecise levels of impulses for T_i -parameter CS.

As shown in the above figures, the highest deviation of filter response is caused by the erroneous level of the second impulse of CS. The T_i -parameter signals are more sensitive to imprecise levels of impulses with the exception of the last impulse, for which the filter response alters in the same manner for both types of CSs.

4. EXPERIMENTAL VERIFICATION OF THE METHOD

Verification of simulation research for α -parameter and T_i -parameter CSs was carried out in an exemplary electronic embedded system equipped with an ADuC814 microcontroller [4]. During the experimental verification the low-pass Butterworth filters, whose parameters are shown in Table 1, were the subject of investigations.

4.1 The embedded system used for verification

The block diagram of the electronic embedded system is presented in Fig. 12.

The ADuC814 runs at a clock frequency of exactly 2.097152 MHz. Durations of CS impulses are precisely ascertained by the 16-bit Timer0 with a resolution of 5.72 μ s.

The timer interrupt subroutine modifies registers of Timer0 and DAC0.

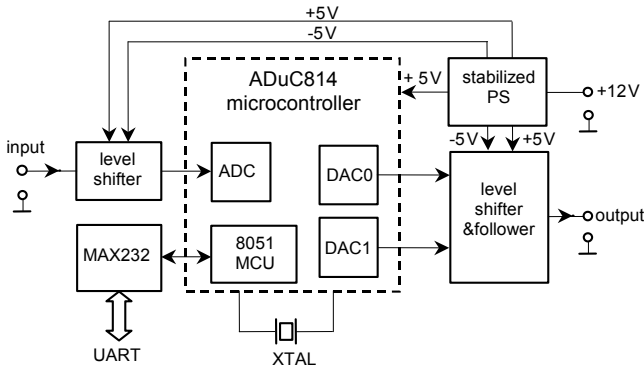


Fig. 12. The electronic embedded system for experimental verification of the method for CSs.

The ADC used for measuring the CUT response has a full-scale range of 2.5V. However, both DACs used for generating of CSs have a full-scale range of 5V.

Because the microcontroller is equipped with 12-bit unipolar AD and DA converters, the level shifters are required for processing bipolar signals. The input signal is shifted to a 1.235V reference level provided by a LM385-1.2 voltage reference diode. Thus, the adjusted reference level allows to measure signals with the amplitude of $\pm 1.235V$. The generated CS is shifted to a reference level of $-2.5V$ provided by DAC1 to obtain the bipolar output CS with levels up to $\pm 2.5V$. The DAC1 output voltage is adjusted in order to get a 0V output level in the no-signal state.

4.2 The practical realization of tested filters

The examined filters of 2nd (4th) order were realized with one (two) UAF42 [5]. The UAF42 is a universal active filter that can be configured for a wide range of two-pole low-pass, high-pass, and band-pass filters. It uses a classic state-variable analog architecture with an inverting amplifier and two integrators (Fig. 13).

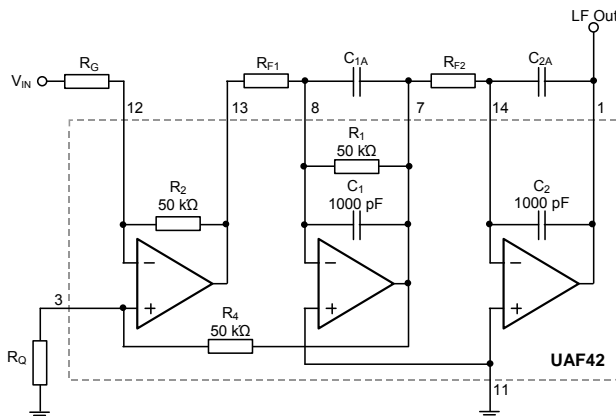


Fig. 13. The 2nd order low-pass filter realized with UAF42 circuit.

The UAF42 filter analog structure allows independent modification of the Q -factor (adjusted by the value of resistor R_0) and the cut-off angular frequency ω_n (adjusted simultaneously by the values of R_{F1} and R_{F2} resistors),

which was desired. Both investigated Butterworth filters have a cut-off frequency of 10 Hz.

4.3 The results of experimental verification

During the experimental verification the influence of following factors on tested filters response has been examined: deviation of ω_n and Q -factor, duration of the first impulse of CS and improper values of impulse levels.

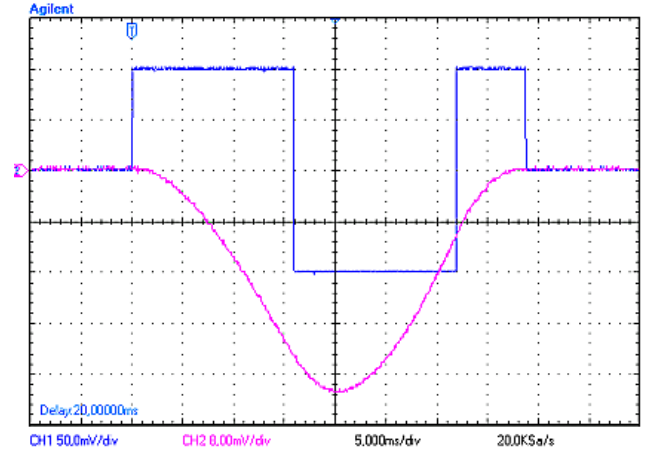


Fig. 14. The CUT response to matched T_T -parameter CS.

The oscillogram of stimulation and response of the examined 2nd order filter to matched T_T -parameter CS is shown in Fig. 14. The filter response reaches zero and remains at that level after the end of stimulation t_f , which confirms the result of simulation research.

The next figures present two exemplary oscillograms of responses of the examined Butterworth low-pass filters with non-nominal values of parameters ω_n and Q -factor. The first oscillogram (Fig. 15) demonstrates the response of the 2nd order filter for $\Delta\omega_n/\omega_n = -50\%$ to α_T -parameter CS. The second one (Fig. 16) shows the response of the 4th order filter to T_T -parameter signal for $\Delta Q_2/Q_2 = 50\%$, where Q_2 is the Q -factor of the filter's second section.

The non-zero filters responses after ending of stimulations, caused by displacement of transfer function poles, are visible in both oscillograms.

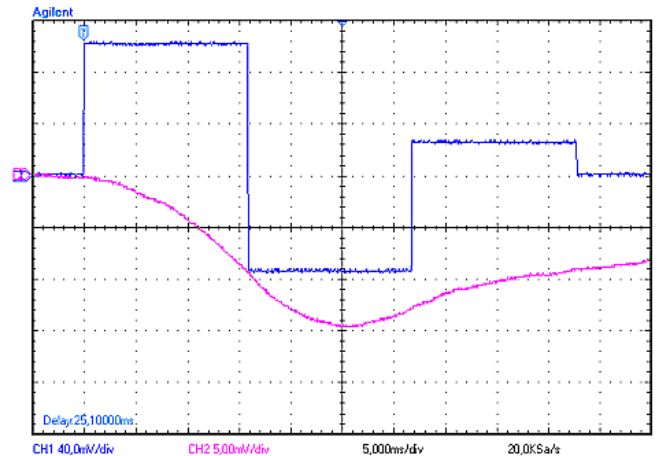


Fig. 15. The response of 2nd order filter for $\Delta\omega_n/\omega_n = -50\%$ to α_T -parameter CS.

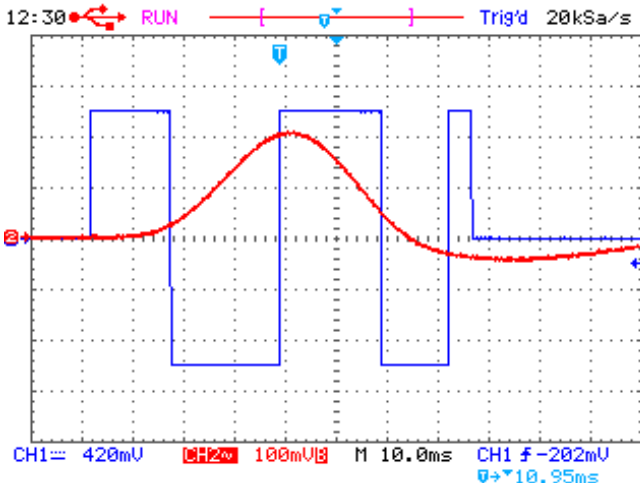


Fig. 16. The response of 4th order filter for $\Delta Q_2/Q_2=50\%$ to T_I -parameter CS.

The plots of absolute errors of responses

$$\varepsilon_y = y_m(t_f) - y_s(t_f) \quad (10)$$

where: $y_m(t_f)$ – measured response,
 $y_s(t_f)$ – simulated response,

in the moment t_f for the 4th order filter stimulated with both types of CSs are shown in Fig. 17 for alteration of Q -factors and Fig. 18 for alteration of cut-off angular frequencies ω_n for both filter sections.

The maximal absolute error does not exceed the value of several millivolts for any parameter or type of CS.

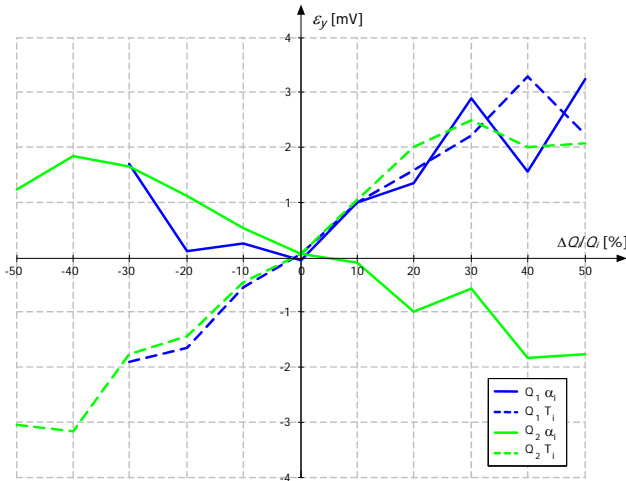


Fig. 17. The absolute error of response ε for the 4th order filter and variable Q -factors of both sections.

Comparisons between results obtained from experimental verification $y_m(t_f)$ and simulation research $y_s(t_f)$ for the 2nd order filter are mentioned below in Tables 4-7. The absolute error of the examined 2nd order filter response ε_y does not exceed the level of several millivolts, which is similar as for the 4th order filter.

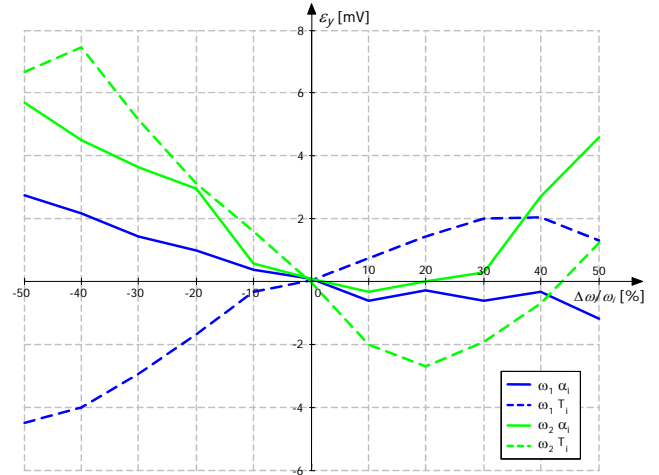


Fig. 18. The absolute error of response ε for the 4th order filter and variable cut-off angular frequencies ω_n of both sections.

Table 4. Measured and simulated response of the 2nd order filter for variable Q -factor and α -parameter signal.

$\Delta Q/Q$ [%]	Q	$y_m(t_f)$ [mV]	$y_s(t_f)$ [mV]	ε_y [mV]
-30	0.495	-23.5	-24.5	1
-20	0.566	-15	-15.86	0.86
-10	0.636	-7	-7.62	0.62
0	0.707	0	0	0
10	0.778	6	6.9	-0.9
20	0.849	11.5	13.07	-1.57
30	0.919	17	18.55	-1.55
40	0.990	21	23.39	-2.39
50	1.061	25.5	27.65	-2.15

Table 5. Measured and simulated response of the 2nd order filter for variable Q -factor and T_I -parameter signal.

$\Delta Q/Q$ [%]	Q	$y_m(t_f)$ [mV]	$y_s(t_f)$ [mV]	ε_y [mV]
-30	0.495	2	1.12	0.88
-20	0.566	2.5	2.06	0.44
-10	0.636	2	1.57	0.43
0	0.707	0	-0.01	0.01
10	0.778	-1.5	-2.42	0.92
20	0.849	-4	-5.43	1.43
30	0.919	-7.5	-8.86	1.36
40	0.990	-11	-12.58	1.58
50	1.061	-14	-16.47	2.47

Table 6. Measured and simulated response of the 2nd order filter for variable ω_n parameter and α -parameter signal.

$\Delta \omega_n / \omega_n$ [%]	ω_n [rad/s]	$y_m(t_f)$ [mV]	$y_s(t_f)$ [mV]	ε_y [mV]
-50	31.416	-90	-92.85	2.85
-40	37.699	-87	-90.9	3.9
-30	43.982	-76	-78.28	2.28
-20	50.265	-57	-57.07	0.07
-10	56.549	-31	-30	-1
0	62.832	-3	0	-3
10	69.115	26	30.18	-4.18
20	75.398	53	58.14	-5.14
30	81.681	76	82	-6
40	87.965	93	100.4	-7.4
50	94.248	104	112.53	-8.53

Table 7. Measured and simulated response of the 2nd order filter for variable ω_n parameter and T_i -parameter signal.

$\Delta\omega_n/\omega_n$ [%]	ω_n [rad/s]	$y_m(t_f)$ [mV]	$y_s(t_f)$ [mV]	ε_y [mV]
-50	31.416	-79	-83.41	4.41
-40	37.699	-81	-86.1	5.1
-30	43.982	-74	-78.47	4.47
-20	50.265	-58	-60.79	2.79
-10	56.549	-32	-34.12	2.12
0	62.832	0	-0.01	0.01
10	69.115	38	39.64	-1.64
20	75.398	80	82.85	-2.85
30	81.681	122	127.63	-5.63
40	87.965	167	172.15	-5.15
50	94.248	208	214.75	-6.75

The influence of erroneous levels of CSs impulses on the deviation of the fault-free circuit response was verified experimentally. The absolute errors of the examined filter response ε_y are shown in Fig. 19 and Fig. 20 for both type of CSs.

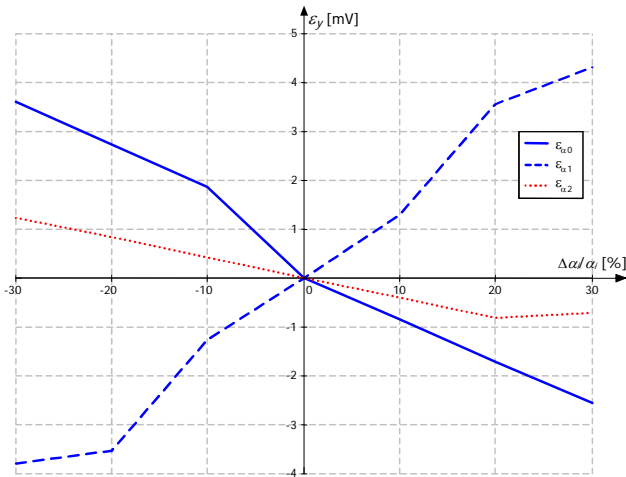


Fig. 19. The absolute error of response ε_y for variable $\Delta\alpha_i/\alpha_i$ and α_i -parameter CS.

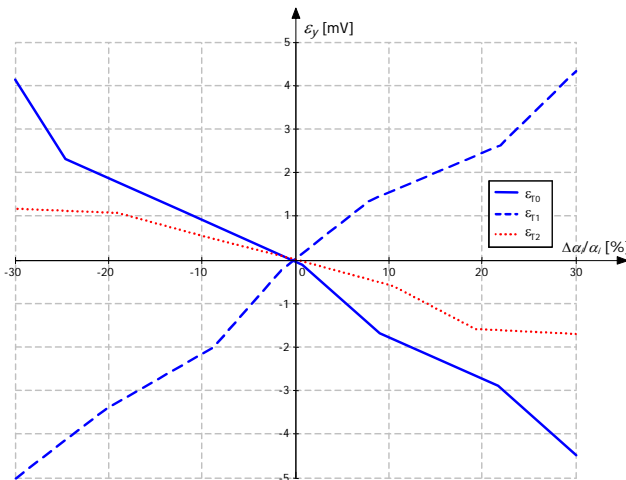


Fig. 19. The absolute error of response ε_y for variable $\Delta\alpha_i/\alpha_i$ and T_i -parameter CS.

The difference between response values gained from simulations and measurements) does not exceed the level of 5 mV for $-30\% < \Delta\alpha_i/\alpha_i < 30\%$ and both types of CS.

5. CONCLUSION

The presented diagnostic method for testing of analog circuits basing on CSs can be applied to BISTs in mixed-signal electronic embedded systems. This approach requires nothing more than internal peripherals of the system microcontroller and only 300 bytes of its free program memory for creating the CS BIST.

The method transfers complicated processing of a CUT response to the synthesis of a specially shape designed CS that is matched to the tested object. In consequence the CUT response processing is extremely simple and fast.

The class of tested objects is limited to circuits whose frequency characteristics are determined by poles of their transfer functions. The presented method is predestined for diagnostics of analog circuits in the range of low and very low frequencies, where a short testing time is gained in comparison with other diagnostic methods.

The parameters of utilized α_i -parameter signals can be easily computed analytically, however for T_i -parameter signals the estimation is more complicated, because simultaneous non-linear equations have to be solved with application of numerical computations. The technical realization of of T_i -parameter signal generator is easier in comparison to an α_i -parameter one since a DAC with a resolution of at least 10 bits is required.

T_i -parameter CSs are more sensitive to inaccuracy of their parameters during generation, but they provide a higher level of CUT response for a given fault in comparison to α_i -parameter signals.

The optimal stimulating CS should be selected in pre-test phase for a given transfer function of the tested circuit. T_i -parameter CSs allow to increase the method's sensitivity at the cost of a longer testing time, which is not possible for α_i -parameter signals.

The presented CSs permit to test analog circuits with split power supply lines. At present, a new class of unipolar complementary signals, which are predestined for testing of analog circuits with single supply, are examined.

REFERENCES

- [1] Bartosiński B., Zielonko R., "New classes of complementary signals", *Electronic Letters*, Vol. 23, No. 9, pp. 433-434, 1987.
- [2] B. Bartosiński, "Method of testing linear electronic circuits with the aid of T_i -parameters complementary signals", *Metrology and Measurements Systems* 16, pp. 389-396, 1993. (in Polish)
- [3] Schreiber H., "Fault dictionary based upon stimulus design", *IEEE Transaction on Circuits and Systems*, Vol. Cas-26, No. 7, pp. 529-537, July 1979.
- [4] Analog Devices, "ADuC814 Microconverter®", datasheet PDF file, www.analog.com, 2003.
- [5] Burr-Brown, "The UAF42 universal active filter - Application Bulletin", PDF file, www.burr-brown.com, 1993.